

Theoretical Study of Solvent-Exchange Reactions on Hexasolvated Divalent Cations in the First Transition Series: Model Calculation of a Hydrogen Cyanide Exchange

Yuko Wasada-Tsutsui, Hiroaki Wasada,*,† and Shigenobu Funahashi††

Institute of Natural Sciences, Nagoya City University, Mizuho-ku, Nagoya 467-8501

†Faculty of Regional Studies, Gifu University, Gifu 501-1193

††Laboratory of Analytical Chemistry, Graduate School of Science, Nagoya University, Nagoya 464-8602

Received February 3, 2003; E-mail: wasada@cc.gifu-u.ac.jp

The stability of divalent cations (M(II)) of the first transition series, penta-, hexa-, and heptasolvated by hydrogen cyanide was studied in order to clarify the reaction mechanisms of nitrile-exchange reactions. The structural stabilities of the $[M(NCH)_7]^{2+}$s depend on the d-electron configurations, though all of the $[M(NCH)_5]^{2+}$s and $[M(NCH)_6]^{2+}$s are located at the local minima. The $[M(NCH)_7]^{2+}$s are structurally more stable than the heptahydrated analogues. Successive binding energies show that it is difficult for an incoming ligand to penetrate the first solvation shells of cations in the later members. Thus, the associative mechanism of solvent-exchange reactions is favorable for cations in the earlier members resulting from energetics as well as structural stability. The symmetry of the imaginary vibrational mode along the reaction path corresponds to that of the transition density induced by one-electron excitation from the antibonding orbital occupied in the d^3 ion to the 4s orbital. The stable $[M(NCH)_7]^{2+}$s arise from the large excitation energies sufficient to reduce the second term (see Eq. 4 in the text) of Bader–Pearson's second-order perturbation expansion.

Ligand-substitution reactions of metal complexes are important to clarify the nature of the chemical bonds of the coordination compounds. Usually, these reactions progress in aqueous solution due to the high solvability of water. Recently, metal ions dissolved in organic solvents have been studied because of their interesting catalytic behavior in organic reactions. An organic solvent, which can dissolve many electrolytes, must have a high dielectric constant. Moreover, aprotic solvents favor organic reactions which are sensitive to protons. Acetonitrile has a relatively high dielectric constant of 36,[1] and is widely used to dissolve electrolytes and to study electrode reactions.

The metal ion in solution is directly coordinated by a certain number of solvent molecules that construct the first solvation shell. In aqueous solution, the hydration number of the di- and trivalent cations in the first transition series is six, when we take into account of the axial water molecules of a tetragonally distorted octahedron by the Jahn–Teller effect.[2] According to recent studies of metal ions in organic solvents, the coordination numbers of these ions significantly depend on the bulkiness of the groups around the coordinating atoms in the solvent molecules. Some divalent cations of the first transition series are six-coordinated in organic solvents without bulky groups, such as acetonitrile.[3]

Solvating molecules are always displaced from the first coordination shell by free solvent molecules in bulk. This very simple process is the so-called solvent-exchange reaction, which is regarded as being a standard of all ligand substitution reactions on a metal ion because of its simplicity. The reaction mechanisms of solvent exchanges are similar to any other ligand substitution proceeding in solution, which is competitive with the solvent-exchange reactions. Because water-exchange reactions have been experimentally investigated for most metal ions, sufficient trends have been found to estimate the reaction mechanisms.[4] Theoretical studies of these reactions clarify the stereochemistries and electronic structures of their reaction paths by using a cluster model that contains a metal ion and water molecules entering and coordinating in the first hydration shell.[5,6] For the solvent-exchange reactions in organic solvents, some experimental studies are known.[3]

The mechanisms of the ligand substitution reactions are classified on the basis of the coordination number and structural stability of their intermediary species.[7] In the dissociative (D) mechanism, an intermediate with a reduced coordination number is formed by cleavage of the bond between the leaving ligand and the central metal ion. In the associative (A) mechanism, an intermediate with an expanded coordination number is formed by the coordination of the entering ligand. The interchange mechanism has a transition state instead of an intermediate. The interchange mechanism is further classified according to the degree of bond breaking in the transition state. In the transition state for the dissociative-interchange (I_d) mechanism, the degree of bond breaking between the leaving ligand and the metal ion is greater than that of the bond making between the entering ligand and the metal ion, and vice versa for the associative-interchange (I_a) mechanism. The activation mode of the solvent-exchange reactions on octahedrally hexacoordinated divalent and trivalent cations var-

Published on the web September 15, 2003; DOI 10.1246/bcsj.76.1713

ies from I_a for the earlier members to I_d for the later members of the first transition series.

Theoretical investigations of the water-exchange processes on divalent and trivalent ions in the first transition series show that the reaction mechanisms depend on the structural stability of the heptacoordinated species placed on the associative mechanisms.[5d,5e,6] The d-electron configurations of these heptahydrated metal ions determine the potential curvature along the reaction path, though the pentahydrated and hexahydrated metal ions are located at local minima. The heptahydrated metal ions are located at local minima, or saddle points, if they have less than 8 d electrons, while the rest are located at second-order saddle points, which cannot connect any associative reaction paths. This results in associative mechanisms that can operate for water exchanges on metal ions having less than 8 d electrons, while dissociative mechanisms are feasible for all members in the first transition series.

We studied the solvent-exchange reactions on divalent cations of the first transition series in nitriles using ab initio molecular orbital methods. Their reaction mechanisms have been experimentally investigated. We used a cluster model containing hydrogen cyanide molecules and a metal cation.[8] We also examined which electronic structures of the heptacoordinated species dominate the reaction mechanism, like the water-exchange processes. We discuss here the ligand effect on the structural stabilities and the reaction mechanisms, while comparing previous studies concerning the water-exchange reactions.[6]

Experimental

Computational Details. We determined the structures of hexasolvated divalent cations ($[M(NCH)_6]^{2+}$; M = Ca, Sc, Ti, V, Cr, Mn, Fe, Co, Ni, Cu, and Zn), heptasolvated divalent cations ($[M(NCH)_7]^{2+}$), and pentasolvated divalent cations ($[M(NCH)_5]^{2+}$); these are modeled on the initial, associative intermediary, and dissociative intermediary species, respectively. We considered high-spin cations because high-spin Mn(II), Fe(II), and Co(II) ions are experimentally known in acetonitrile solution. We characterized the structural stabilities by frequency calculations to discuss the operative reaction mechanisms in a manner similar to previous discussions on the water-exchange reactions.[6]

We calculated the total binding energy (Eq. 1) to estimate the energetics of the solvent-exchange reaction,

$$M^{2+} + n\mathrm{HCN} \rightarrow [M(NCH)_n]^{2+}$$
$$(M = \mathrm{Ca, Sc, Ti, V, Cr, Mn, Fe, Co, Ni, Cu, and Zn}, n = 5, 6, 7). \quad (1)$$

The basis set superposition errors (BSSE) between M^{2+} and the solvent molecules were estimated by the Boys–Bernardi counterpoise method.[9] The successive binding energies were calculated by the difference between the n th and $(n-1)$-th solvation energies (Eqs. 2 and 3),

$$[M(NCH)_6]^{2+} + \mathrm{HCN} \rightarrow [M(NCH)_7]^{2+}, \quad (2)$$

$$[M(NCH)_6]^{2+} \rightarrow [M(NCH)_5]^{2+} + \mathrm{HCN}. \quad (3)$$

All of the calculations of the closed and open-shell systems were carried out at the RHF and UHF level, respectively, using a full double-zeta plus polarization basis set. For the central cations, the [8s4p3d] segmented contraction of the (14s9p5d) primitive sets of Wachters[10a] was used. The s and p spaces were contracted using the contraction number I, while the d space was contracted to [311]. For calcium, three even-tempered d functions ($\alpha = 1.378, \alpha = 0.446, \alpha = 0.144$)[10b] were used. The Huzinaga–Dunning [4s2p]/(9s5p) basis set for the first-row atoms and [2s]/(4s) for hydrogen were used. The basis set of hydrogen was scaled by a factor of 1.2. Two 4p functions of Wachters scaled by a factor of 1.5 were added to the basis set of a central cation, and d polarization functions were added to the basis sets of carbon and nitrogen ($\alpha_C = 0.75$, $\alpha_N = 0.8$). Åkesson et al. performed CASSCF calculations with all five 3d orbitals as the active space for the hexahydrated titanium(III), cobalt(II), and iron(II) ions in order to examine the non-dynamical correlation effect for this type of open-shell system.[5a,b] They showed that the hydration energies, given by CASSCF and SCF, were not significantly different and concluded that the mixing of states was merely an atomic effect. Therefore, we carried out electronic structure calculations of open-shell systems at the UHF level. For heptahydrated divalent cations, the dynamical electron correlation shortens the bonds between the central cation and a water molecule by 0.04–0.07 Å.[6b,c] The back-donation from the central cation to the CN triple bond is expected to shorten the ion–ligand bond. We also performed geometry optimization for $[M(NCH)_6]^{2+}$ (M = Mn, Ni, and Cu) and calculated the total binding energies of $[M(NCH)_7]^{2+}$ at the MP2 level to examine the dynamical correlation effect on the molecular structure and energetics.

We used the Gaussian 98 program[11] on an SGI ORIGIN 2000, IBM SP, and DEC-Alpha for all of the ab initio molecular-orbital calculations and the MOLCAT program[12] on a Macintosh for visualizing the molecular structures and vibrational modes. The contour maps and isosurfaces of the molecular orbitals were drawn using the MOPLOT and MOVIEW programs.[13] We discuss the energy in kcal mol^{-1} (1 kcal mol^{-1} is 4.1884 kJ mol^{-1}) and in atomic units (a.u., 1 a.u. = 627.50959 kcal mol^{-1}) and bond lengths in Å (1 Å = 100 pm).

Results and Discussion

Hexa(hydrogen cyanide) Divalent Cations; Initial State. The structures, the electronic properties, and the lowest vibrational frequency of the $[M(NCH)_6]^{2+}$s are given in Table 1. All of the hexasolvated species are located at the local minima. The coordination geometries of closed and half-closed shell ions (d^0 Ca(II), d^3 V(II), d^5 Mn(II), d^8 Ni(II), and d^{10} Zn(II)) are strictly octahedral. The coordination octahedra of other ions with partially filled shells are distorted by the Jahn–Teller effect. Tetragonal elongation occurs along a four-fold axis in the d^1 Sc(II) ion as well as the d^4 Cr(II) and d^9 Cu(II) ions, whereas a $[Sc(H_2O)_6]^{2+}$ is trigonally compressed.[14] The coordination octahedra of the Ti(II) and Fe(II) ions are slightly tetragonally compressed. A $[Co(NCH)_6]^{2+}$ is trigonally compressed; the bond angles between adjacent Co–N bonds equivalent in the three-fold axis are 91.0°, and the other bond angles between adjacent Co–N bonds are 89.0°. A large d–π interaction between the central cation and N–C triple bonds favors the tetragonal distortions. This is especially remarkable in the earlier member ions having spread and high-energy 3d orbitals.

The experimental bond lengths between the central ion and N of $[Mn(NCCH_3)_6]^{2+}$, $[Ni(NCCH_3)_6]^{2+}$, and $[Cu(NCCH_3)_6]^{2+}$ for the equatorial and the axial bonds in acetoni-

Table 1. Metal–Nitrogen Bond Lengths, Electronic Properties, and Harmonic Vibrational Frequencies for $[M(NCH)_6]^{2+}$

Metal	M–N distance/Å[b]		Total Energy/a.u.[c]	$\langle S^2\rangle$[d]	Freq. /cm^{-1} [e]
	(equatorial)	(axial)			
Ca	2.522		−1233.869322	0.000	41.1
Sc	2.395	2.401	−1316.844382	0.760	44.2
Ti	2.328	2.327	−1405.499405	2.014	50.8
V	2.261		−1499.971913	3.776	62.1
Cr	2.217	2.472	−1600.348118	6.041	48.5
Mn	2.316		−1706.849044	8.752	47.7
Fe	2.255	2.254	−1819.414698	6.007	54.2
Co[a]	2.216		−1938.347945	3.756	56.2
Ni	2.170		−2063.778305	2.008	65.4
Cu	2.114	2.351	−2195.818235	0.754	57.4
Zn	2.198		−2334.660494	0.000	57.3

a) D_{3d} structure. b) 1 Å = 100 pm. c) 1 a.u. = 2628.3 kJ mol^{-1}. d) Total squared-magnitude of the spin. e) 1 cm^{-1} = 1.98648×10^{-23} J.

trile solutions are 2.22, 2.07, 1.99, and 2.23 Å, respectively.[3] The calculated bond lengths are longer than experimental ones by 0.1 Å. A previous study of Ag(I) ion solvated by hydrogen cyanide or acetonitrile suggested that the presence of methyl groups shortens the Ag–N bonds by less than 0.02 Å.[8] The shorter experimental bond lengths do not arise from neglecting the methyl groups in the model systems, but from the dynamical correlation and the polarization of ligands by the second-solvation shell. The ion–N bond lengths of $[M(NCH)_6]^{2+}$s, calculated at the MP2 level, are 2.268 Å, 2.105 Å, 2.302 Å, and 2.051 Å for Mn(II), Ni(II), Cu(II) axial bonds and Cu(II) equatorial bonds, respectively. The ion–N bonds, calculated at the MP2 level, are shorter than those at the Hartree–Fock level by 0.04–0.06 Å. For $[M(H_2O)_7]^{2+}$s, the M–O bond shortenings at the MP2 level are 0.04–0.07 Å, and do not differ seriously among the cations in the first transition series.[6b,c] We expected that the dynamical correlation shortens the ion–N bonds almost the same as hydrated cations for all of the cations in the first transition series.

Hepta(hydrogen cyanide) Divalent Cations; Associative Mechanism. The structures, the electronic properties, and the lowest vibrational frequency of the $[M(NCH)_7]^{2+}$s are given in Table 2. The transition vectors correspond to the concerted entering and leaving motions of adjacent hydrogen cyanides with N_4 and N_5, on a V(II) or a Ni(II) ion, the so-called cis-attack. For a Ni(II) ion, the entering and leaving hydrogen cyanides with N_2 and N_3 are placed on the opposite side of a Ni(II) ion, the so-called trans-attack (see Fig. 1). The intrinsic reaction coordinate of the solvent-exchange reaction on the V(II) ion is plotted as a function of the distance between V and N_5 of the leaving ligand in Fig. 2. The heptacoordinated structure is the transition state on the intrinsic reaction coordinate of the solvent exchange on a $[V(NCH)_6]^{2+}$. The activation energy is 17.7 kcal mol^{-1} (see Fig. 2), which is larger than that of the water exchange (14.6 kcal mol^{-1}).[6d] The V–N bond lengths are different between the hexasolvated species shown in Fig. 2 (GR, 2.234 Å) and listed in Table 1 (2.261 Å). In Table 1, we treat an isolated $[V(NCH)_6]^{2+}$, while in Fig. 2 we show $[V(NCH)_6]^{2+}\cdot$NCH, which has an extra solvent (the entering ligand) in the second solvation shell. There is a hydrogen-bond between the extra solvent and the first solvation shell ligand (the leaving ligand) for $[V(NCH)_6]^{2+}\cdot$NCH case. The hydrogen bonded HCN is polarized and closer to the central cation. The entering ligand reaches near the final position of the reaction much earlier than does the leaving ligand. This is the reason why the potential surface falls steeply near the product region. The structure and the two imaginary modes of $[Cu(NCH)_7]^{2+}$ located at a second-order saddle point are shown in Fig. 3. These imaginary modes are degenerate; one is antisymmetric stretching, corresponding to the solvent-exchange reaction mode, and the other is symmetric stretching related to the simultaneous elimination of two ligands.

The $[M(NCH)_7]^{2+}$s with d^0, d^1, and d^2 configrations are located at the local minima, the d^3 ion is located at the saddle point, the d^4, d^5, d^6, and d^7 ions are located at the local minima, the d^8 ion is located at the saddle point, the d^9 ion is located at the second-order saddle point, and the d^{10} ion is located at a local minimum, whereas the heptahydrated d^4, d^6, and d^7 ions are located at saddle points and d^8 and d^{10} ions are located at second-order saddle points.[5d,5e,6] Furthermore, from a comparison of the imaginary frequencies between $[M(NCH)_7]^{2+}$s and $[M(H_2O)_7]^{2+}$s, we can say that the curvatures along the reaction coordinate tend to be positive for the $[M(NCH)_7]^{2+}$s (for example, the imaginary frequencies of $[V(NCH)_7]^{2+}$ and $[V(H_2O)_7]^{2+}$ are 95.4i and 128.7i cm^{-1}, respectively). It is considered that the associative mechanism can operate for hydrogen cyanide exchange on the $[M(NCH)_6]^{2+}$s in the first transition series, except for the Cu(II) ion, due to the presence of heptasolvated species connected to the reaction coordinate. This result is quite different from the $[M(H_2O)_6]^{2+}$s in the reaction mechanisms for Ni(II) and Zn(II), where only the dissociative mechanisms can operate for water exchange.

The pentagonal bipyramid and the capped trigonal prism are known as regular coordination geometries of heptacoordination compounds. These geometries are related to each other in a simple way. If the plane defined by two adjacent equatorial ligands is tilted in a pentagonal bipyramid, a capped trigonal prism is formed (see Scheme 1). Therefore, the deviation from the pentagonal bipyramid is measured with the tilt angle related to the dihedral angle between the planes defined by the metal ion, N_1, and N_2 retained on the equatorial plane and by the metal ion, N_1, and N_4 on the tilted plane, i.e., the dihedral angle of N_4–metal ion–N_1–N_2. The dihedral angle of a pentagonal bipyramid is 0°, and that of a capped prism is 45°. For the $[M(NCH)_7]^{2+}$s, the tilt angles are very small for all the ions, except for the Ti(II) and Co(II), whereas the heptahydrated ions favor a capped prism except for Ni(II). Especially, the coordination geometries of ions with a closed or half-closed d-shell are perfect pentagonal bipyramids. On the other hand, the coordination geometry of $[Ti(NCH)_7]^{2+}$ is a capped prism. For $[Co(NCH)_7]^{2+}$, the distortion of the equatorial plane is symmetric to the plane containing N_1 and the axial bonds, i.e., N_2 and N_3 are displaced downward and N_4 and N_5 are displaced upward.

In pentagonal bipyramids of the $[M(NCH)_7]^{2+}$s, the axial coordinate bonds are shorter than the equatorial ones. The

Table 2. Metal–Nitrogen Bond Lengths, Electronic Properties, and Harmonic Vibrational Frequencies for $[M(NCH)_7]^{2+}$

	Ca(II)	Sc(II)	Ti(II)	V(II)	Cr(II)	Mn(II)
d electron number	0	1	2	3	4	5
Electronic state	$^1A_1'$	^2A	^3A	^4B	^5A	$^6A_1'$
Point group	D_{5h}	C_1	C_1	C_2	C_1	D_{5h}
Bond length[a]						
M–N_1	2.607	2.493	2.428	2.299	2.356	2.465
M–N_2	2.607	2.495	2.384	2.341	2.696	2.465
M–N_3	2.607	2.495	2.383	2.341	2.615	2.465
M–N_4	2.607	2.495	2.436	2.704	2.413	2.465
M–N_5	2.607	2.495	2.442	2.704	2.486	2.465
M–N_6	2.527	2.394	2.383	2.243	2.172	2.283
M–N_7	2.527	2.394	2.384	2.243	2.172	2.283
Dihedral angle[b]	0.0	0.0	48.2	0.2	0.0	0.0
Total energy[c]	−1326.777107	−1409.750110	−1498.400827	−1592.854749	−1693.244373	−1799.745585
$\langle S^2\rangle$[d]	0.0000	0.7582	2.0099	3.7665	6.0123	8.7523
Frequency[e]	16.5	23.6	4.2	95.4*i*	11.6	22.9
	Fe(II)	Co(II)	Ni(II)	Ni(II)	Cu(II)	Zn(II)
d electron number	6	7	8	8	9	10
Electronic state	$^5B_2$	^4A	$^3B_1$	$^3A_1$	$^2A_1'$	$^1A_1'$
Point group	C_{2v}	C_1	C_{2v}	C_{2v}	D_{5h}	D_{5h}
Bond length[a]						
M–N_1	2.467	2.395	2.225	2.209	2.440	2.408
M–N_2	2.377	2.377	3.027	2.204	2.440	2.408
M–N_3	2.377	2.377	3.027	2.204	2.440	2.408
M–N_4	2.426	2.409	2.156	2.885	2.439	2.408
M–N_5	2.426	2.410	2.156	2.885	2.439	2.408
M–N_6	2.218	2.171	2.119	2.104	2.030	2.107
M–N_7	2.218	2.174	2.119	2.104	2.030	2.107
Dihedral angle[b]	0.0	−26.6, 27.0	0.0	0.0	0.0	0.0
Total energy[c]	−1912.307366	−2031.236320	−2156.657478	−2156.658123	−2288.707313	−2427.547269
$\langle S^2\rangle$[d]	6.0071	3.7560	2.0064	2.0066	0.7527	0.0000
Frequency[e]	6.3	3.6	100.0*i*	79.2*i*	65.1*i*, 65.1*i*	14.9

a) In Å. 1 Å = 100 pm. The numbers of N atoms are shown in Fig. 1. b) In degree. A dihedral angle is an angle between planes defined by M, N_4 and N_5, and by M, N_2 and N_3. c) In atomic unit. 1 a.u. = 2628.3 kJ mol^{-1}. d) Total squared-magnitude of the spin. e) In cm^{-1}. 1 cm^{-1} = 1.98648×10^{-23} J. For a structure at a local minimum, the lowest real frequency is given. For a structure at a saddle point or second-order saddle point, all the imaginary frequencies are given.

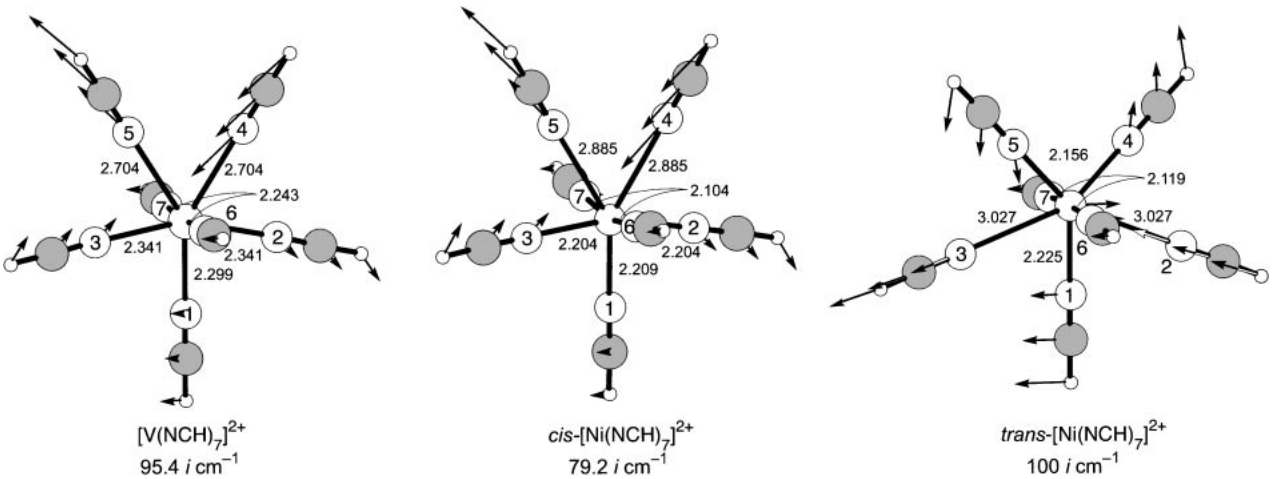

Fig. 1. The optimized structures and transition vectors of $[V(NCH)_7]^{2+}$ and $[Ni(NCH)_7]^{2+}$. The numbers on nitrogen atoms show numbering used in the text and the Table 2.

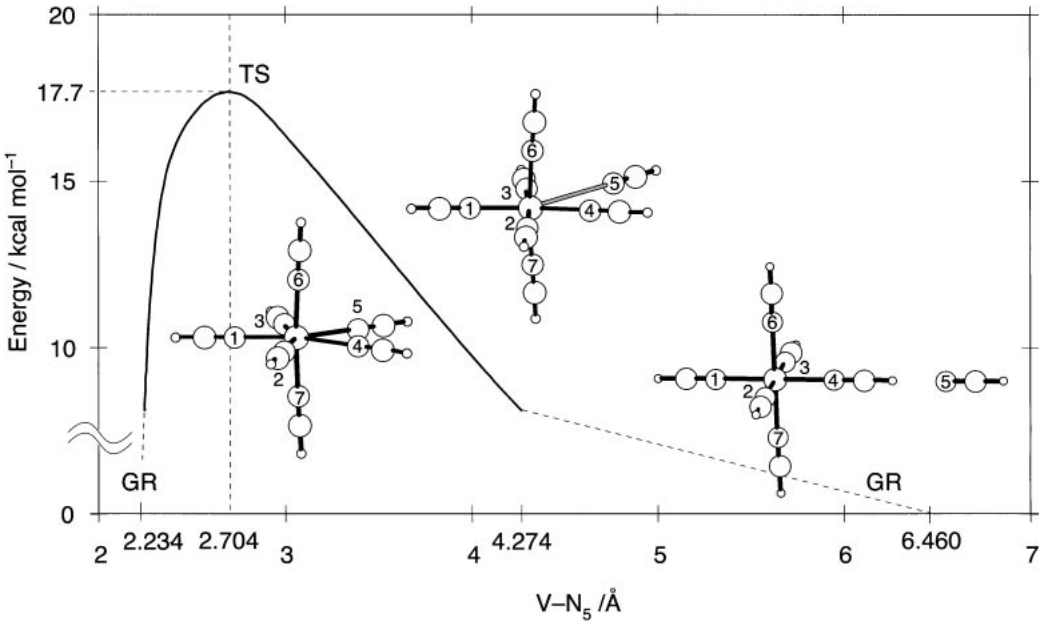

Fig. 2. The intrinsic reaction coordinate for hydrogen cyanide exchange on $[V(NCH)_6]^{2+}$. A potential energy curve plotted against the distance between the V(II) ion and N_5 of the leaving (or entering) ligand. GR and TS are abbreviations for ground and transition state, respectively.

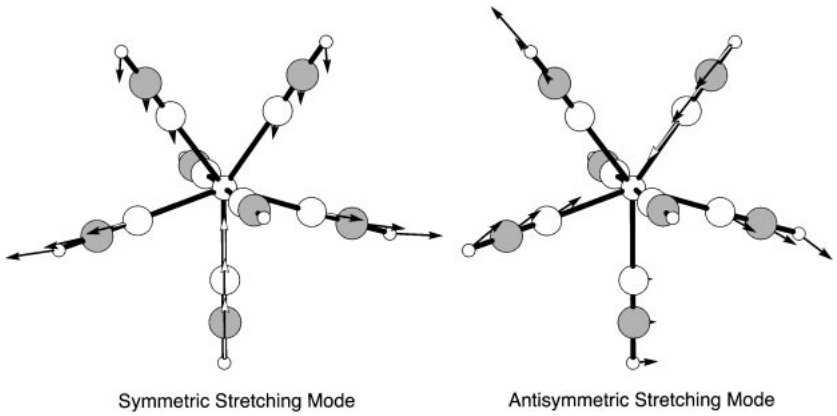

Fig. 3. The two imaginary vibrational modes of $[Cu(NCH)_7]^{2+}$. These are degenerate and their frequencies are $65.1i$ cm^{-1}.

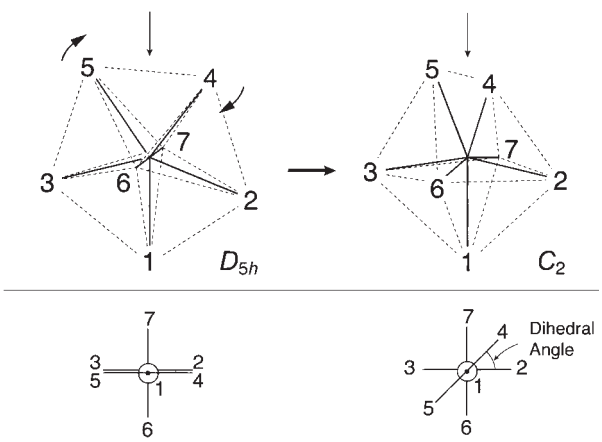

Scheme 1.

$[Cu(NCH)_7]^{2+}$ and $[Zn(NCH)_7]^{2+}$ have axial bonds shorter than the equatorial ones by 0.4 Å and 0.3 Å (see Table 2); it thus seems that these solvated ions are linear dicoordinate and surrounded by five weakly coordinating ligands. Moreover, the axial bond length of all the $[M(NCH)_7]^{2+}$s, except for the Ca(II) and Ti(II) ions, are shorter than those of the $[M(NCH)_6]^{2+}$s. In comparison with the $[M(H_2O)_7]^{2+}$s, the $[M(NCH)_7]^{2+}$s of the earlier members have coordinate bonds longer by 0.02–0.05 Å and the Ca(II) ion has coordinate bonds longer by 0.07 Å, while the Co(II), Cu(II), and Zn(II) ions of the later members have shorter axial coordinate bonds. In conclusion, the $[M(NCH)_7]^{2+}$s prefer the pentagonal bipyramidal coordination geometry with short axial bonds.

Penta(hydrogen cyanide) Divalent Cations; Dissociative Mechanism. The structures, the electronic properties, and the lowest vibrational frequencies of the $[M(NCH)_5]^{2+}$s are given in Table 3. All of the $[M(NCH)_5]^{2+}$s are located at the local minima in the same manner as $[M(NCH)_6]^{2+}$s. This

Table 3. Metal–Nitrogen Bond Lengths, Electronic Properties, and Harmonic Vibrational Frequencies for $[M(NCH)_5]^{2+}$

Metal	Coordination geometry[a)]	Equatorial/ basal[b)]	Axial/ apex[b)]	Total energy /a.u.	$\langle S^2 \rangle$	Frequency /cm^{-1}
Ca	TBP	2.488	2.498	−1140.938142	0.000	19.7
Sc	(TBP)	2.370, 2.353	2.379	−1223.910791	0.758	19.9
Ti	TBP	2.295	2.333, 2.289	−1312.563839	2.013	15.7
V	SQP	2.237	2.218	−1407.033462	3.775	45.9
Cr	SQP	2.191	2.369	−1507.427080	6.019	36.0
Mn	TBP	2.246	2.289	−1613.922145	8.754	21.3
Fe	(TBP)	2.189, 2.183	2.231	−1726.487010	6.007	20.7
Co	TBP	2.153	2.223, 2.152	−1845.419999	3.756	29.0
Ni	SQP	2.129	2.098	−1970.847925	2.007	35.8
Cu	SQP	2.091	2.203	−2102.898958	0.754	17.9
Zn	TBP	2.100	2.189	−2241.738806	0.000	35.0

a) TBP and SQP are abbreviations of trigonal bipyramidal and square pyramidal, respectively. Parentheses of (TBP) mean that equatorial bonds' angles of TBP are quite different from ideal 120° (the angles are 106° for Sc(II) and 110° for Fe(II)). Two long and one short equatorial bonds are found in (TBP). b) Metal–nitrogen bond lengths are in Å. 1 Å = 100 pm.

indicates that the dissociative mechanism is possible to operate for the hydrogen cyanide exchange reactions on all of these ions. Though almost all of the $[M(NCH)_5]^{2+}$s have coordinate-bonds shorter than those of the $[M(NCH)_6]^{2+}$s, $[M(NCH)_5]^{2+}$s' bending modes lower than the hexasolvated species suggest flexible geometries. The typical coordination geometries of the pentacoordinate compounds are the trigonal bipyramid and the square pyramid, which can be interconverted by a pseudorotation process. The actual geometry is intermediary and sensitive to the d-electron configurations. The square pyramidal geometries of the $[V(NCH)_5]^{2+}$, $[Cr(NCH)_5]^{2+}$, $[Ni(NCH)_5]^{2+}$, and $[Cu(NCH)_5]^{2+}$ can avoid unfavorable occupancy of anti-bonding orbitals. The $[Sc(NCH)_5]^{2+}$ and $[Fe(NCH)_5]^{2+}$ have intermediate coordination geometries due to the large deviation of the equatorial bond angles from 120°. The coordination geometries of the $[M(NCH)_5]^{2+}$s are similar to those of the $[M(H_2O)_5]^{2+}$s reported by Åkesson et al.,[5b] except for the Sc(II) and Fe(II) ions having the intermediate coordination geometries.

Solvation Energy and Energetics of Intermediary Species. Table 4 lists the total and successive binding energies of the $[M(NCH)_5]^{2+}$s, $[M(NCH)_6]^{2+}$s, and $[M(NCH)_7]^{2+}$s in order to estimate the energetics of the stationary points on the reaction paths.[15] The total binding energies give the absolute stabilities of the associative and dissociative intermediary species. On the other hand, the successive binding energies give their stabilites relative to the hexasolvated initial states, and suggest tendencies for a ligand to penetrate or to leave from a first solvation shell along an associative or a dissociative pathway, respectively.

The total binding energies of the later members of the first transition series are greater than the earlier ones, since they are reflected by an increase in the effective nuclear charge. The energies of the hexasolvated ions have maxima at the d^3 and d^8 configurations, as expected from crystal field theory, while those of the $[M(NCH)_5]^{2+}$s and $[M(NCH)_7]^{2+}$s have maxima at d^4 and d^9 inspite of occupying antibonding orbitals. The trend in the total binding energies for the $[M(NCH)_5]^{2+}$s and $[M(NCH)_6]^{2+}$s is the same as for the those of $[M(H_2O)_6]^{2+}$s,[5a,5c] while the heptahydration energies have maxima at d^3 and d^8.[6c] The total binding energies for heptasolvation by hydrogen cyanide are greater than heptahydration by

Table 4. Total and Successive Binding Energies of $[M(NCH)_5]^{2+}$, $[M(NCH)_6]^{2+}$, and $[M(NCH)_7]^{2+}$ a)

	Total binding energy[b)]			Successive binding energy	
	$[M(NCH)_6]^{2+}$	$[M(NCH)_7]^{2+}$	$[M(NCH)_5]^{2+}$	c)	d)
Ca	−251.1	−264.3	−226.0	−13.2	25.1
Sc	−278.3	−289.7	−251.4	−11.3	27.0
Ti	−293.9	−304.0	−266.0	−10.1	27.9
V	−314.0	−311.2	−283.5	2.8	30.5
Cr	−307.7	−312.9	−288.5	−5.3	19.1
Mn	−299.6	−305.2	−276.7	−5.6	23.0
Fe	−316.3	−319.5	−292.7	−3.2	23.6
Co	−327.0	−327.7	−303.4	−0.7	23.6
Ni	−342.3	−338.0	−316.7	4.3	25.5
Cu	−340.7	−341.7	−321.8	−1.0	19.0
Zn	−335.9	−336.0	−315.8	−0.1	20.0

a) In kcal mol^{-1}. 1 kcal mol^{-1} = 4.1884 kJ mol^{-1}. b) $M^{2+} + n\mathrm{HCN} \rightarrow [M(NCH)_n]^{2+}$, $n = 5, 6, 7$. c) $[M(NCH)_6]^{2+} + \mathrm{HCN} \rightarrow [M(NCH)_7]^{2+}$. d) $[M(NCH)_6]^{2+} \rightarrow [M(NCH)_5]^{2+} + \mathrm{HCN}$.

a few kcal mol^{-1}, due to the ion–N bonds stronger than the ion–O bonds.

The successive binding energies suggest that the seventh ligand binding energies decrease as one moves to the right in the periodic table, while the decrease in the sixth ligand dissociation energies is ambiguous. It is difficult for a ligand to penetrate the first solvation shells of ions in the later members, while the dissociation of a ligand is slightly enhanced. Thus, the associative mechanism is favorable for solvent-exchange reactions on ions in the earlier members resulting from energetics as well as structural stability. Whether the activation mode is associative or dissociative, high activation energies are expected for the solvent exchange on the V(II) and Ni(II) ions, because of the particularly high stability of the hexasolvated initial states.

Relationship between Structural Stability and Antibonding Orbitals in Hepta(hydrogen cyanide) Species. As shown in Scheme 2, the five 3d orbitals of a central metal cation interact with the lone-pair orbitals of the coordinating hydrogen cyanide molecules and split into two lower non-bonding orbitals (e_1'') and three higher antibonding orbitals (e_2', a_1'). The number of these antibonding orbitals is independent of the changes in the coordination geometry from pentagonal bipyramid to capped prism. Therefore, the bond orders of the coordinate bonds are reduced in the high-spin heptasolvated divalent cations when they have three or more electrons. The effect of the bond order on the coordination geometry is important in $[V(NCH)_7]^{2+}$ where the singly occupied antibonding orbital points toward the longest bonds. The equatorial bond lengths are sensitive to their bond orders, which are varied by occupation of the σ antibonding orbitals.

Transition vectors of the solvent exchange reactions on hexacoordinated ions, as shown in Fig. 1, correspond to antisymmetric stretching modes along the long bonds in the "equatorial plane". According to Bader–Pearson's second-order perturbation theory,[16] when there are vibrational modes of which the symmetry is the same as that of the transition density,[17] these motions induce an energy decrease. Thus, if there is no transition density corresponding to the vibrational mode which destroys the heptacoordination geometries, it can remain as a stable species. An available transition density is induced by one-electron excitation from the antibonding orbital occupied in d^3 ions (ϕ_1) to the 4s unoccupied orbital of the cation, (ϕ_1) × (4s).[6b–d] This transition density on the equatorial plane of $[V(NCH)_7]^{2+}$ is shown in Fig. 4. The transition density between ϕ_1 and an empty d orbital is not concerned with the deformation resulting from a solvent-exchange reaction because it differs in symmetry from the transition vector of the reaction. The large antisymmetric character on N_4 and N_5 corresponds to the transition vectors, like a water-exchange reaction on the V(II) ion. It is expected that the heptahydrated and hepta(hydrogen cyanide) ions should have almost equal structural stabilities, because the orbitals which will make the σ coordination bonds have almost the same orbital energy for a free water and hydrogen cyanide molecules, compared with an ammonia molecule having a lone pair on the N atom (Scheme 3).

However, the $[M(NCH)_7]^{2+}$s are more structurally stable than the heptahydrated analogues. At a stationary point, the potential energy is expanded in terms of a set of normal coordinates $\{Q_i\}$ (Eq. 4).

$$E_0 = E_0^{(0)} + Q\left\langle \Psi_0^{(0)} \middle| \left(\frac{\partial U}{\partial Q}\right)_0 \middle| \Psi_0^{(0)} \right\rangle + \frac{Q^2}{2}\left\langle \Psi_0^{(0)} \middle| \left(\frac{\partial^2 U}{\partial Q^2}\right)_0 \middle| \Psi_0^{(0)} \right\rangle + Q^2 \sum_{k\neq 0} \frac{\left| \left\langle \Psi_0^{(0)} \middle| \left(\frac{\partial U}{\partial Q}\right)_0 \middle| \Psi_k^{(0)} \right\rangle \right|^2}{E_0^{(0)} - E_k^{(0)}} + o(Q^3) \quad (4)$$

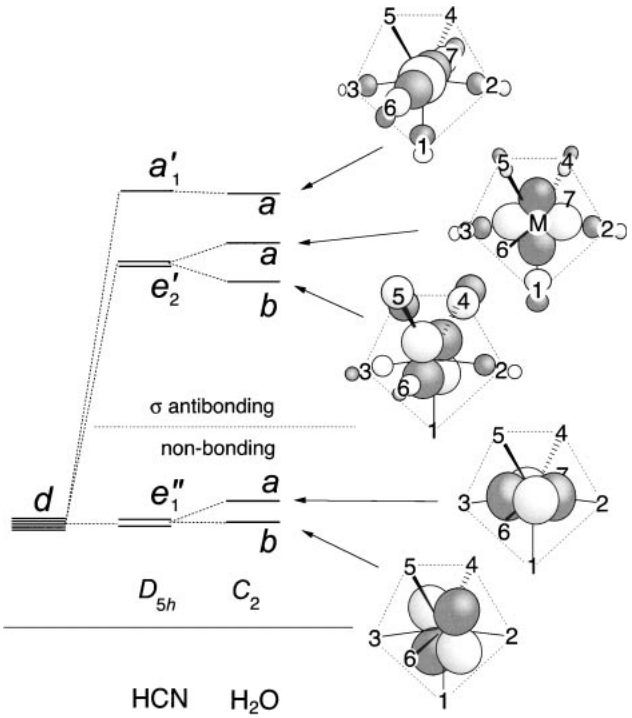

Scheme 2.

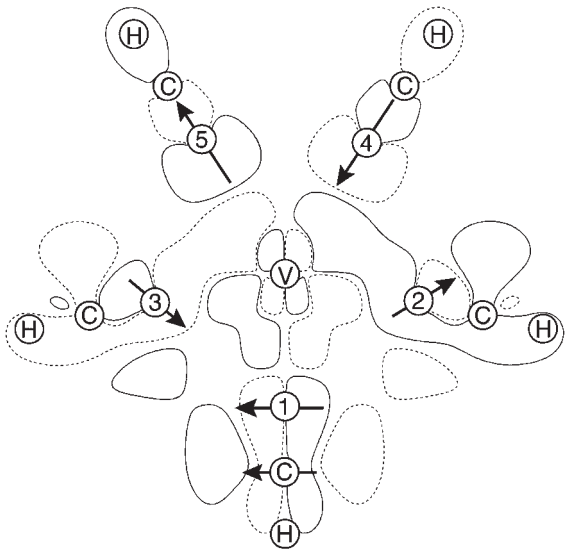

Fig. 4. The transition density between the σ-anti-bonding and the 4s-type orbitals of the central cation on the equatorial plane of $[V(NCH)_6]^{2+}$. Positive regions are surrounded with solid lines and negative regions are surrounded with dashed lines. The transition vectors correspond to arrows from positive to negative regions.

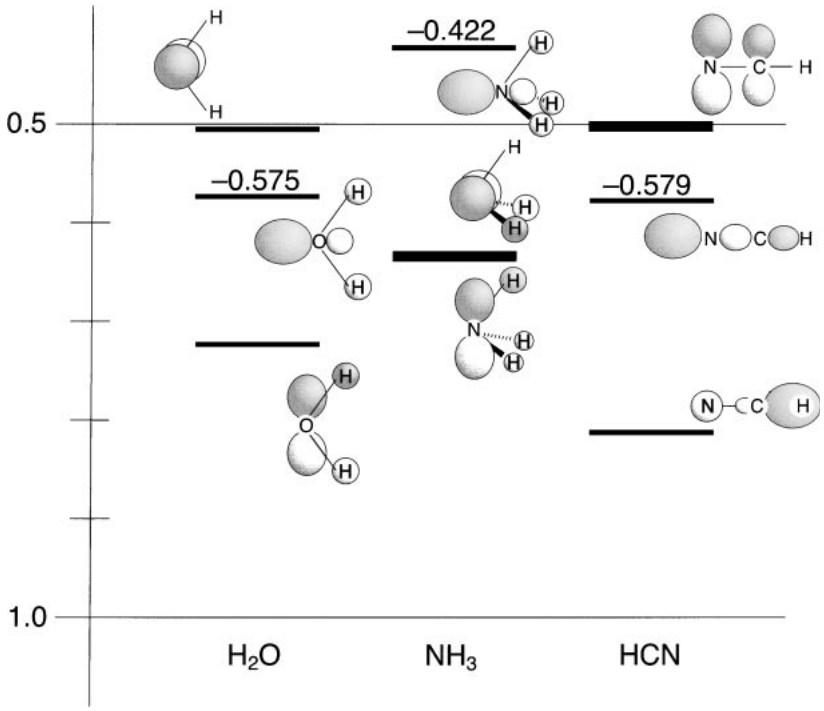

Scheme 3.

The stable structures of the $[M(NCH)_7]^{2+}$s arise from the less-negative second terms, which prevent deformation along the reaction coordinate. The negative terms are less effective if the denominators, i.e., excitation energies, are large. In Fig. 5, the CI-single excitation energies related to the transition densities are plotted versus the atomic number of the central cations.[18] $[M(NCH)_7]^{2+}$s have large excitation energies sufficient to reduce the effects of the second term than in the case of $[M(H_2O)_7]^{2+}$s. $[Cr(NCH)_7]^{2+}$ and $[Fe(NCH)_7]^{2+}$ have the lowest normal vibration modes corresponding to the concerted motion of the solvent exchange, and are structurally more stable than the heptahydrated analogue, while the lowest normal vibration mode of $[Mn(NCH)_7]^{2+}$, whose hexahydrated analogue is at a local minimum, is not concerned with a solvent exchange.

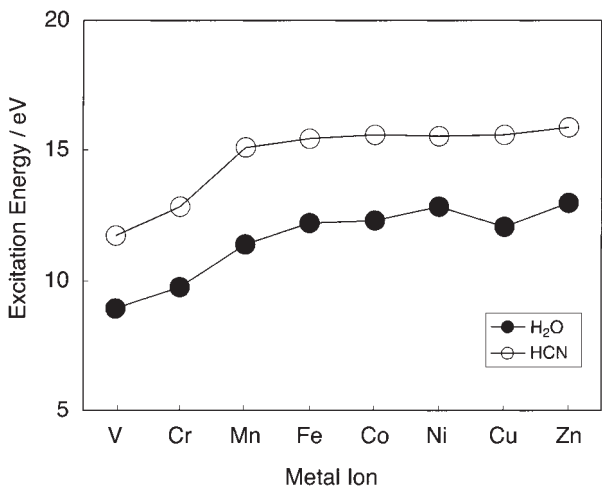

Fig. 5. One-electron excitation energies from the σ-antibonding and the 4s-type orbitals for $[M(H_2O)_7]^{2+}$ and $[M(NCH)_7]^{2+}$. 1 eV = 86.485 kJ mol^{-1}. A $[M(H_2O)_7]^{2+}$ has a lower excitation energy than a $[M(NCH)_7]^{2+}$.

Though both the 4s orbitals and the antibonding orbitals in $[M(NCH)_7]^{2+}$s are higher in energy than the $[M(H_2O)_7]^{2+}$s, the energy promotion of the 4s orbitals is slightly greater than the antibonding orbitals, because of electron repulsions between a diffuse 4s electron and π electrons on the ligands. This induces the higher excitation energies in the $[M(NCH)_7]^{2+}$s than those in the heptahydrated ones. It is expected that the structural stability should be reduced for the divalent cations heptasolvated by alkyl cyanides where the inductive effect of the alkyl groups increase the orbital energy of the N lone pair.

We have also found that a $[Cr(H_2O)_7]^{2+}$ has a less-negative potential energy curvature than a $[V(H_2O)_7]^{2+}$.[6b] The common feature in these heptasolvated Cr(II) ions is shorter axial bonds by 0.1 Å than the heptasolvated V(II) and Mn(II) ions. These shorter axial bonds arise from the unique unoccupied orbital directed to axial bonds, and cause a large orbital interaction in this direction of the heptasolvated Cr(II) ions. As shown in Scheme 4, via the influence of the ligand orbitals, the empty $3d_{z^2}$ orbital mixes with the 4s orbital so that the equatorial part of the 4s orbital shrinks. Table 5 lists the degrees of the mixing and the second-order energy lowering $E(2)$[19] between the $3d_{z^2}$ and 4s orbitals. $E(2)$ is also related to the destabilization energy of the upper orbital. The n and $E(2)$ values of the $[Cr(NCH)_7]^{2+}$ are larger than those of $[V(NCH)_7]^{2+}$ and $[Mn(NCH)_7]^{2+}$. This makes the $[Cr(NCH)_7]^{2+}$ stable, such that the excitation energy from the σ antibonding orbital to the 4s orbital is large. On the other hand, $[Cu(NCH)_7]^{2+}$ is located at a second-order saddle point. It is expected that the orbital interaction between the $3d_{z^2}$ and 4s orbitals is not large enough to make the $[Cu(NCH)_7]^{2+}$ stable, because of the large separation between the $3d_{z^2}$ orbital and ligand ones due to the

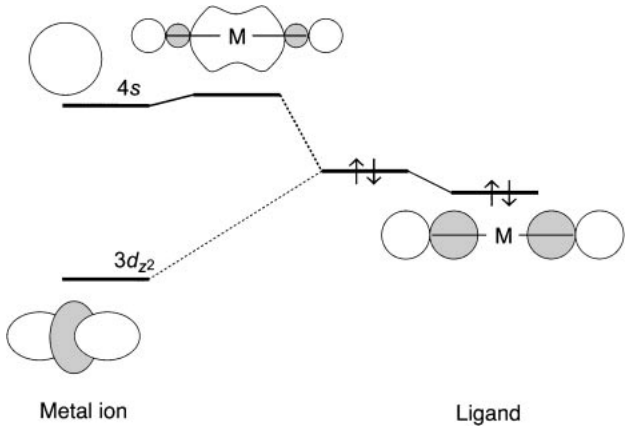

Scheme 4.

Table 5. The 4s Orbital Centered on a Metal Ion Analysed by Natural Population Analysis[a)]

Ion	n in sd^n	$E(2)$[b)]	$\Delta\mathcal{E}$[c)]	F[d)]
		kcal mol^{-1}	a.u.	a.u.
V	0.03	16.83	1.39	0.199
Cr	0.06	19.47	1.29	0.206
Mn	0.00	12.39	1.20	0.160

a) Natural bond orbitals of the 4s orbital centered on the metal ion and an N lone pair orbital for the 6th axial ligand. b) The second-order energy lowering of orbital mixing. c) Orbital energy differences from the acceptor 4s to the donor N lone pair. d) Fock matrix elements between the acceptor 4s and donor N lone pair.

large effective nuclear charge of a Cu(II) ion (Cr(II) is 1.718 and Cu(II) is 1.727 as natural atomic charges).

Conclusions

We studied the stability of the hexasolvated divalent cations ($[M(NCH)_6]^{2+}$; M = Ca–Zn), heptasolvated cations ($[M(NCH)_7]^{2+}$), and pentasolvated cations ($[M(NCH)_5]^{2+}$), which are modeled on initial, associative intermediary, and dissociative intermediary species, respectively, in order to explain the reaction mechanisms for the solvent-exchange reactions in nitrile.

1. Though all of the $[M(NCH)_5]^{2+}$s and $[M(NCH)_6]^{2+}$s are located at local minima, the structural stabilities of the $[M(NCH)_7]^{2+}$s strongly depend on the d electron configurations. The divalent cations heptasolvated by hydrogen cyanide are structurally more stable than the heptahydrated analogues. Only a $[Cu(NCH)_7]^{2+}$ is located at a second-order saddle point. Dissociative mechanisms are a possible activation mode for the solvent exchange on the divalent cations of all the first transition series, while associative mechanisms are operative for solvent exchange on the divalent cations, except for the Cu(II) ion.

2. The successive binding energies show that it is difficult for an incoming ligand to penetrate the first solvation shell of cations in the later members. Thus, the associative mechanism of the solvent exchange reactions is favorable for ions in the earlier members resulting from energetics as well as structural stability.

3. The symmetry of the imaginary vibrational mode along the reaction path corresponds to the symmetry of the transition density induced by one-electron excitation from the antibonding orbital occupied in the d^3 ions to the 4s orbital. These excitation energies are greater than the $[M(H_2O)_7]^{2+}$s to reduce the second term of Bader–Pearson's second-order perturbation expansion. It is expected that the structural stability should be reduced for divalent cations heptasolvated by alkylnitriles due to the inductive effect of the alkyl groups, and that a possible activation mode for the alkylnitrile exchanges should be more dissociative than hydrogen cyanide exchanges.

The calculations in this work were performed on the IBM SP and ORIGIN 2000 computers of the Computer Center of Nagoya City University. We thank Prof. H. Tatewaki for useful discussions. This work was supported partially by Research Fellowships of the Japan Society for the Promotion of Science for Young Scientist and Grants-in-Aid for Scientific Research on Priority Area (Material Design and Reaction Control by Molecular Physical Chemistry) from the Ministry of Education, Culture, Sports, Science and Technology.

References

1 J. A. Riddick, W. B. Bunger, and T. K. Sakano, "Organic Solvents: Physical Properties and Methods of Purification," 4th ed, John Wiley & Sons, New York (1986).

2 H. Ohtaki and T. Radnai, *Chem. Rev.*, **93**, 1157 (1993).

3 a) M. Ishii, S. Funahashi, K. Ishihara, and M. Tanaka, *Bull. Chem. Soc. Jpn.*, **62**, 1852 (1989). b) Y. Inada, T. Sugata, K. Ozutsumi, and S. Funahashi, *Inorg. Chem.*, **37**, 1886 (1998). c) Y. Inada and S. Funahashi, *Anal. Sci.*, **13**, 373 (1997). d) S. Funahashi and Y. Inada, *Bull. Chem. Soc. Jpn.*, **75**, 1901 (2002).

4 a) A. E. Merbach, *Pure Appl. Chem.*, **59**, 161 (1987). b) R. van Eldik, T. Asano, and W. J. le Noble, *Chem. Rev.*, **89**, 549 (1989).

5 a) R. Åkesson, L. G. M. Pettersson, M. Sandström, Per E. M. Siegbahn, and U. Wahlgren, *J. Phys. Chem.*, **96**, 10773 (1992). b) R. Åkesson, L. G. M. Pettersson, M. Sandström, Per E. M. Siegbahn, and U. Wahlgren, *J. Phys. Chem.*, **97**, 3765 (1993). c) R. Åkesson, L. G. M. Pettersson, M. Sandström, and U. Wahlgren, *J. Am. Chem. Soc.*, **116**, 8691 (1994). d) F. P. Rotzinger, *J. Am. Chem. Soc.*, **118**, 6760 (1996). e) F. P. Rotzinger, *J. Am. Chem. Soc.*, **119**, 5230 (1997). f) M. Hartmann, T. Clark, and R. van Eldik, *J. Am. Chem. Soc.*, **119**, 7843 (1996). g) M. Hartmann, T. Clark, and R. van Eldik, *J. Phys. Chem. A*, **103**, 9899 (1999). h) M. A. Lee, N. W. Winter, and W. H. Casey, *J. Phys. Chem.*, **98**, 8641 (1994). i) R. J. Deeth and L. I. Elding, *Inorg. Chem.*, **35**, 5019 (1996). j) Th. Kowall, P. Caravan, H. Bourgeois, L. Helm, F. P. Rotzinger, and A. E. Merbach, *J. Am. Chem. Soc.*, **120**, 6569 (1998).

6 a) Y. Tsutsui, H. Wasada, and S. Funahashi, *Bull. Chem. Soc. Jpn.*, **70**, 1813 (1997). b) Y. Tsutsui, H. Wasada, and S. Funahashi, *Bull. Chem. Soc. Jpn.*, **71**, 73 (1998). c) Y. Tsutsui, H. Wasada, and S. Funahashi, *Bull. Chem. Soc. Jpn.*, **71**, 1771 (1998). d) Y. Tsutsui, H. Wasada, and S. Funahashi, *J. Mol. Struct.: THEOCHEM*, **461–462**, 379 (1999).

7 C. N. Langford and H. B. Gray, "Ligand Substitution Processes," Benjamin, Inc., New York (1966).

8 Hydrogen cyanide as a protic solvent is quite different from aprotic nitriles such as acetonitrile, because the former pro-

duces cyanide anion in solution but the latter does not. However, proton transfers in the present cluster model are meaningless because the model has no proton acceptor such as a solvent. Moreover, we have already showed that the difference between hydrogen cyanide and acetonitrile is small in solvation energy to Ag(I) ions. For further details, see: Y. Tsutsui, K. Sugimoto, H. Wasada, Y. Inada, and S. Funahashi, *J. Phys. Chem. A*, **101**, 2900 (1997).

9 S. F. Boys and F. Bernardi, *Mol. Phys.*, **19**, 553 (1970).

10 a) A. J. H. Wachters, *J. Chem. Phys.*, **52**, 1033 (1970). b) S. Huzinaga, J. Andzelm, M. Klobukowski, E. Radzio-Andzelm, Y. Sakai, and H. Tatewaki, "Physical Sciences Data 16: Gaussian Basis Sets for Molecular Calculations," Elsevier, Amsterdam (1984). c) E. R. Davidson and D. Feller, *Chem. Rev.*, **86**, 681 (1986). d) S. Huzinaga, *J. Chem. Phys.*, **42**, 1293 (1965). e) T. H. Dunning, *J. Chem. Phys.*, **53**, 2823 (1970).

11 M. J. Frisch, G. W. Trucks, H. B. Schlegel, G. E. Scuseria, M. A. Robb, J. R. Cheeseman, V. G. Zakrzewski, J. A. Montgomery, Jr., R. E. Stratmann, J. C. Burant, S. Dapprich, J. M. Millam, A. D. Daniels, K. N. Kudin, M. C. Strain, O. Farkas, J. Tomasi, V. Barone, M. Cossi, R. Cammi, B. Mennucci, C. Pomelli, C. Adamo, S. Clifford, J. Ochterski, G. A. Petersson, P. Y. Ayala, Q. Cui, K. Morokuma, D. K. Malick, A. D. Rabuck, K. Raghavachari, J. B. Foresman, J. Cioslowski, J. V. Ortiz, A. G. Baboul, B. B. Stefanov, G. Liu, A. Liashenko, P. Piskorz, I. Komaromi, R. Gomperts, R. L. Martin, D. J. Fox, T. Keith, M. A. Al-Laham, C. Y. Peng, A. Nanayakkara, C. Gonzalez, M. Challacombe, P. M. W. Gill, B. Johnson, W. Chen, M. W. Wong, J. L. Andres, C. Gonzalez, M. Head-Gordon, E. S. Replogle, and J. A. Pople, "Gaussian 98," Gaussian, Inc., Pittsburgh PA, 1998.

12 Y. Tsutsui and H. Wasada, *Chem. Lett.*, **1995**, 517.

13 a) H. Wasada and Y. Tsutsui, *Bulletin of the College of General Education*, **32**, 153 (1995). b) I. Takahashi, H. Wasada, and Y. Tsutsui, MOVIEW: program of Nagoya University Computer Center representing molecular orbitals and electron density maps by isosurfaces.

14 H. Tachikawa, T. Ichikawa, and H. Yoshida, *J. Am. Chem. Soc.*, **112**, 982 (1990).

15 We estimated effects of the electron correlation on solvation energies by MP2 calculations. Total binding energies of $[M(NCH)_7]^{2+}$ (M = Ca–Zn) are −276.1, −310.3, −328.8, −334.8, −334.0, −324.0, −342.5, −361.3, −363.6, −367.4, and −357.5 kcal/mol. The dynamical electron correlation increases stabilizes of $[M(NCH)_7]^{2+}$s by 10–30 kcal/mol (about 10% of the total binding energies). The stabilization energies arising from the electron correlation have the maximum values at d^2 and d^7. This behavior is similar to the case of stabilization related to d electron configurations. Therefore, the total binding energies of heptasolvation obtained by MP2 and Hartree–Fock calculations depend on the central cations in the almost same way.

16 R. F. W. Bader, *Can. J. Chem.*, **40**, 1164 (1962).

17 The transition density $\rho_{0k}(\boldsymbol{r})$ between the ground state $|\Psi_0{}^{(0)}\rangle$ and an exited state $|\Psi_k{}^{(0)}\rangle$ is defined as follows;

$$\rho_{0k}(\boldsymbol{r}) = \langle\Psi_0{}^{(0)}| - e\sum\nolimits_j \delta(\boldsymbol{r} - \boldsymbol{r}_j)|\Psi_k{}^{(0)}\rangle \quad (5)$$

where $|\Psi_0{}^{(0)}\rangle$ and $|\Psi_k{}^{(0)}\rangle$ are wave functions at a stationary point. A $\rho_{0k}(\boldsymbol{r})$ is given by a product between the orbitals occupied by an excited electron in the ground and excited states, ϕ_i, and ϕ_j, respectively, when Hartree–Fock wave functions are used.

$$\rho_{0k}(\boldsymbol{r}) = c\phi_i{}^*(\boldsymbol{r})\phi_j(\boldsymbol{r}) \quad (c \text{ is a constant}). \quad (6)$$

For further details, see Ref. 16.

18 Because a configuration state function arising from one-electron excitation from the antibonding orbital to the 4s orbital mixes π–π^* transitions and electron transfers from $3d_{z^2}$, we picked up the states having the largest coefficient of the configuration. The correlation coefficient of the excitation energies with the difference between orbital energies related to the excitation is 0.99. The excitation energies are dominantly ruled by the orbital energy differences and relaxation in the excitation has a constant effect on a series of these compounds.

19 a) A. E. Reed, R. B. Weinstock, and F. Weinhold, *J. Chem. Phys.*, **83**, 1164 (1985). b) A. E. Reed, L. A. Curtiss, and F. Weinhold, *Chem. Rev.*, **88**, 899 (1988).